

2009 fall

Phase Transformation of Materials

10.13.2009

Eun Soo Park

Office: 33-316

Telephone: 880-7221

Email: espark@snu.ac.kr

Office hours: by an appointment

Contents for previous class

• Tracer Diffusion in Binary Alloys

D_{Au}^* gives the rate at which Au* (or Au) atoms diffuse in a **chemically homogeneous** alloy, whereas D_{Au} gives the diffusion rate of Au when **concentration gradient** is present.

• High-Diffusivity Paths

$$D_s > D_b > D_l$$



$$A_l > A_b > A_s$$

1. Diffusion along Grain Boundaries and Free Surface

Grain boundary diffusion makes a significant contribution

only when $D_b \delta > D_l d$. ($T < 0.75 \sim 0.8 T_m$)

$$D_{app} = D_l + D_b \frac{\delta}{d}$$

2. Diffusion Along Dislocation

$$D_{app} = D_l + g \cdot D_p$$

At low temperatures, ($T < \sim 0.5 T_m$)

gD_p/D_l can become so large that the apparent diffusivity is entirely due to diffusion along dislocation.

• Diffusion in Multiphase Binary Systems

$$v = \frac{dx}{dt} = \frac{1}{(C_B^b - C_B^a)} \left\{ \tilde{D}(\alpha) \frac{\partial C_B^a}{\partial x} - \tilde{D}(\beta) \frac{\partial C_B^b}{\partial x} \right\}$$

(velocity of the α/β interface)

Contents in Phase Transformation

상변태를
이해하는데
필요한 배경

(Ch1) 열역학과 상태도: **Thermodynamics**

(Ch2) 확산론: **Kinetics**

(Ch3) 결정계면과 미세조직

대표적인 상변태

(Ch4) 응고: **Liquid → Solid**

(Ch5) 고체에서의 확산 변태: **Solid → Solid (Diffusional)**

(Ch6) 고체에서의 무확산 변태: **Solid → Solid (Diffusionless)**

Contents for today's class

Chapter 3 Crystal Interfaces and Microstructure

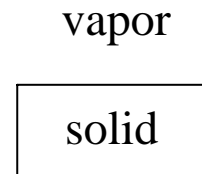
계면의 단순한 형태를 사용하여 계면 자유에너지의 근원을 알아보고 이 계면에너지를 구할 수 있는 몇 가지 방법을 보여줌.

- **Interfacial Free Energy**
- **Solid/Vapor Interfaces**
- **Boundaries in Single-Phase Solids**
 - (a) **Low-Angle and High-Angle Boundaries**
 - (b) **Special High-Angle Grain Boundaries**
 - (c) **Equilibrium in Polycrystalline Materials**

3. Crystal interfaces and microstructure

- Types of Interface

1. Free surface (solid/vapor interface)



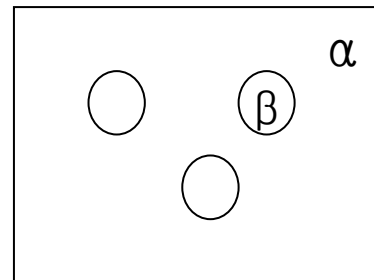
2. Grain boundary (α/α interfaces)

> same composition, same crystal structure

> different orientation

3. inter-phase boundary (α/β interfaces)

> different composition & crystal structure



⇒ defect

⇒ energy ↑

3.1 Interfacial Free Energy

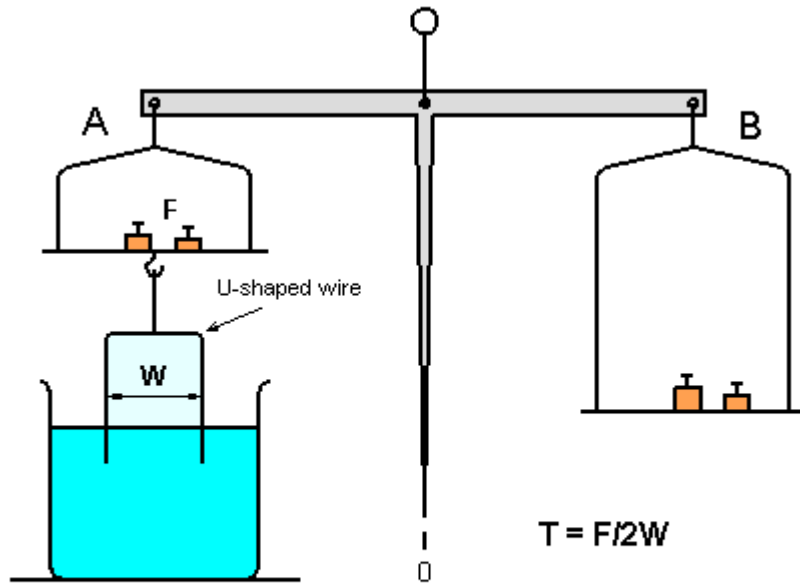
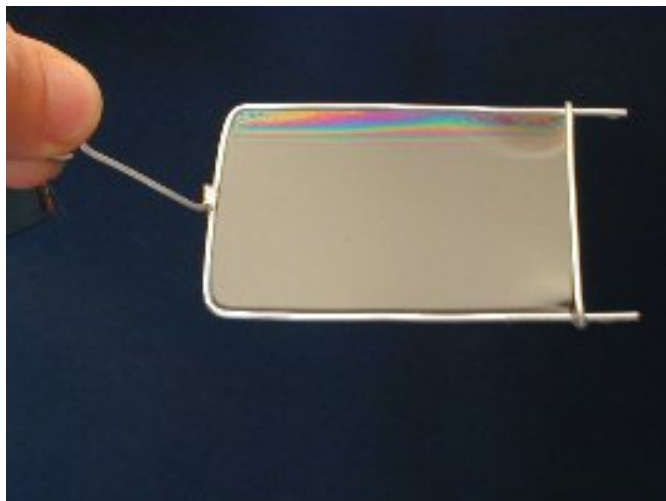


Figure 5 - Experimental device to measure the surface tension of a liquid.



3.1. Interfacial free energy

Interfacial energy (γ) vs. surface tension (F : a force per unit length)

1) work done : $F dA = dG$

2) $dG = \gamma dA + A d\gamma$

$\rightarrow F = \gamma + A d\gamma/dA$

In case of a liq. film, $d\gamma/dA = 0$, $F = \gamma$ (N/m = J/m²)

Ex) liq. : $d\gamma/dA = 0$ Why? **Rearrangement**(채배열)을 통한 일정한 표면구조 유지

sol. : $d\gamma/dA \neq 0$, but, very small value

At near melting temperature $d\gamma/dA = 0$



Fig. 3.1 A liquid film on a wire frame.

3.2 Solid / Vapor Interfaces

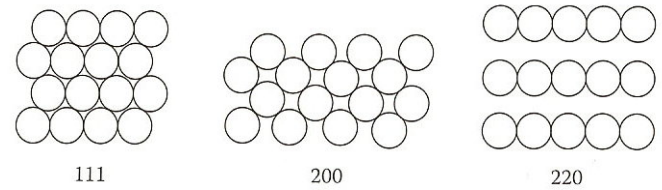
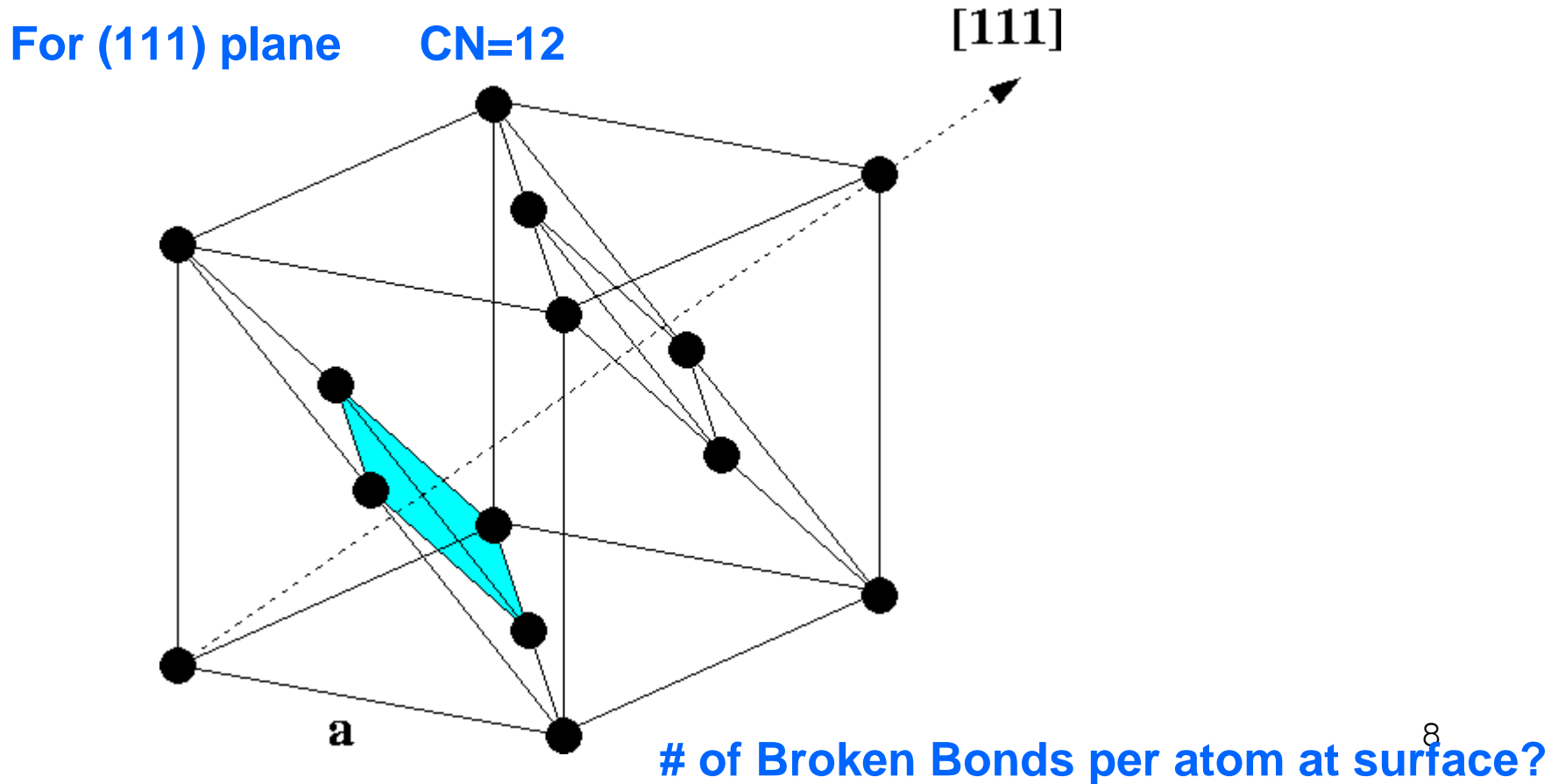


FIGURE 3.2
Atomic configurations on the three closest-packed planes in fcc crystals: (111), (200), and (220)

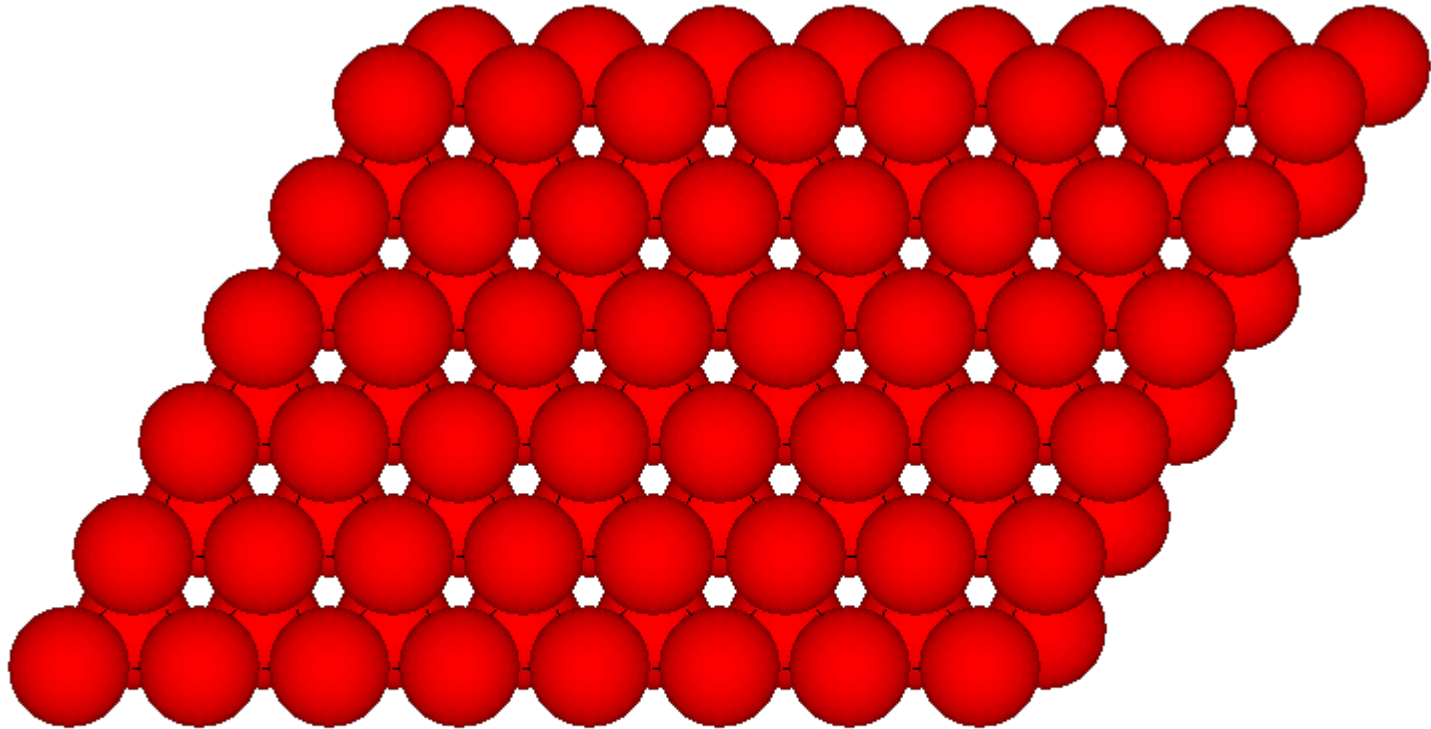
* Hard sphere model

- Fcc : density of atoms in these planes decreases as $(h^2+k^2+l^2)$ increases



of Broken Bonds per atom at surface? → 3 per atom

2005 - S.G. Podkolzin



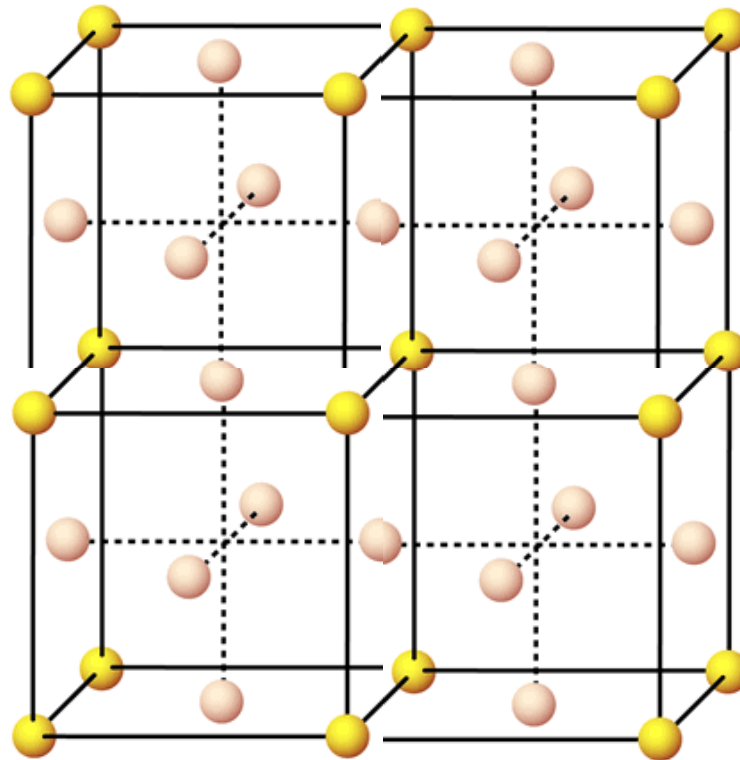
For (111) plane

of broken bond at surface : 3 broken bonds

Bond Strength: $\epsilon \rightarrow$ for each atom : $\epsilon/2$

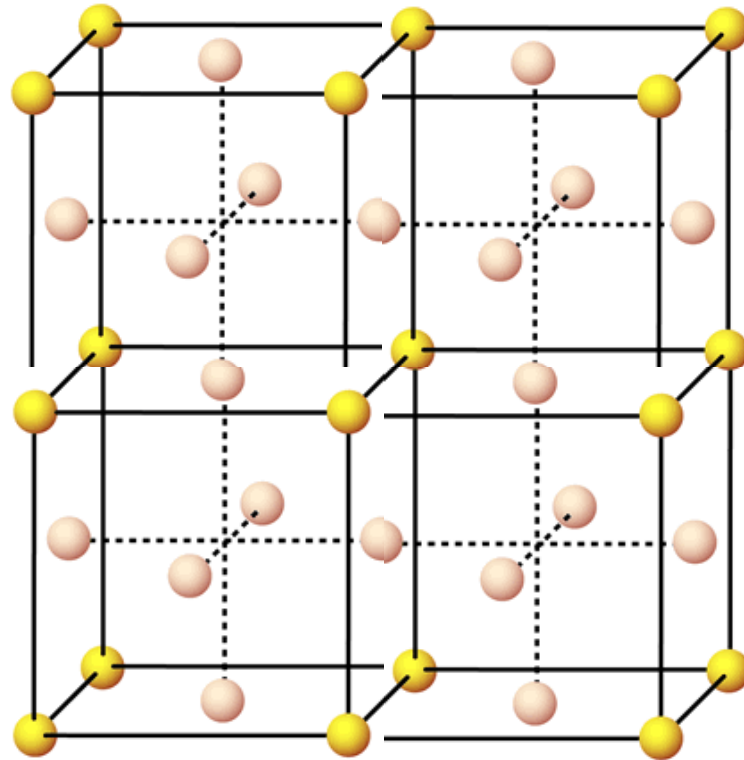
Lowering of Internal Energy per atom on surface: $3\epsilon/2 \downarrow$

For (200) plane CN=12



of Broken Bonds per atom at surface?

For (200) plane CN=12



of Broken Bonds per atom at surface?

of broken bond at surface : 4 broken bonds

Bond Strength: ϵ \rightarrow for each atom : $\epsilon/2$

Lowering of Internal Energy per atom on surface: $4\epsilon/2 \downarrow$

For (100) plane

of broken bond at surface : **3 broken bonds**

Bond Strength: $\epsilon \rightarrow$ for each atom : $\epsilon/2$

Lowering of Internal Energy per atom on surface: $3\epsilon/2$

Heat of Sublimation (승화) in terms of ϵ ? $\rightarrow L_s = 12 N_a \epsilon/2$

Energy per atom of a {111} Surface?

$$E_{sv} = 3 \epsilon/2 = 0.25 L_s / N_a$$

E_{sv} vs γ ?

인접원자들 간의 관계만 고려하여 근사치임.

γ interfacial energy = free energy (J/m²)

$$\rightarrow \gamma = G = H - TS$$

$$= E + PV - TS \quad (: PV \text{ is ignored})$$

$$\rightarrow \gamma = E_{sv} - TS_{sv} \quad (S_{sv} \text{ thermal entropy, configurational entropy})$$

표면>내부

표면에 공공 등의 형성으로 extra S 존재

$$\rightarrow \frac{\partial \gamma}{\partial T} = -S \quad : \text{surface energy decreases with increasing } T$$

$0 < S < 3 \text{ (mJ/m}^2\text{K}^{-1})$ due to increased contribution of entropy

- Average Surface Free Energies of Selected Metals

Crystal	$T_m/^\circ\text{C}$	$\gamma_{sv}/\text{mJ m}^{-2}$
Sn	232	680
Al	660	1080
Ag	961	1120
Au	1063	1390
Cu	1084	1720
δ -Fe	1536	2080
Pt	1769	2280
W	3407	2650

측정 어려움, near T_m

γ of Sn : 680 mJ/m² (T_m : 232°C)

γ of Cu : 1720 mJ/m² (T_m : 1083°C)

C.F. G.B. energy γ_{gb} is about one third of γ_{sv}

Higher T_m

>> stronger bond (large negative bond energy)

>> larger surface energy

- The measured γ values for pure metals near the melting temperature

$$\gamma_{sv} = 0.15 L_s / N_a \quad \text{J / surface atom}$$

$$high T_m \rightarrow high L_s \rightarrow high \gamma_{sv}$$

Surface energy for high or irrational {hkl} index

Closer surface packing > smaller number of broken bond > lower surface energy

표면에서 끊어진 결합수 {111} {200} {220} 면을 따라 증가 > γ_{sv} 면지수 순으로 증가

A crystal plane at an angle θ to the close-packed plane will contain broken bonds in excess of the close-packed plane due to the atoms at the steps.

Surface with high {hkl} index

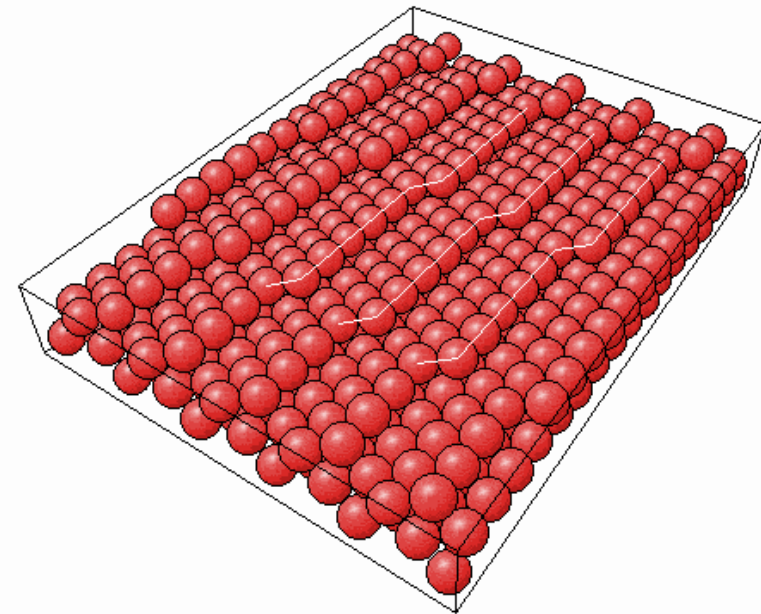
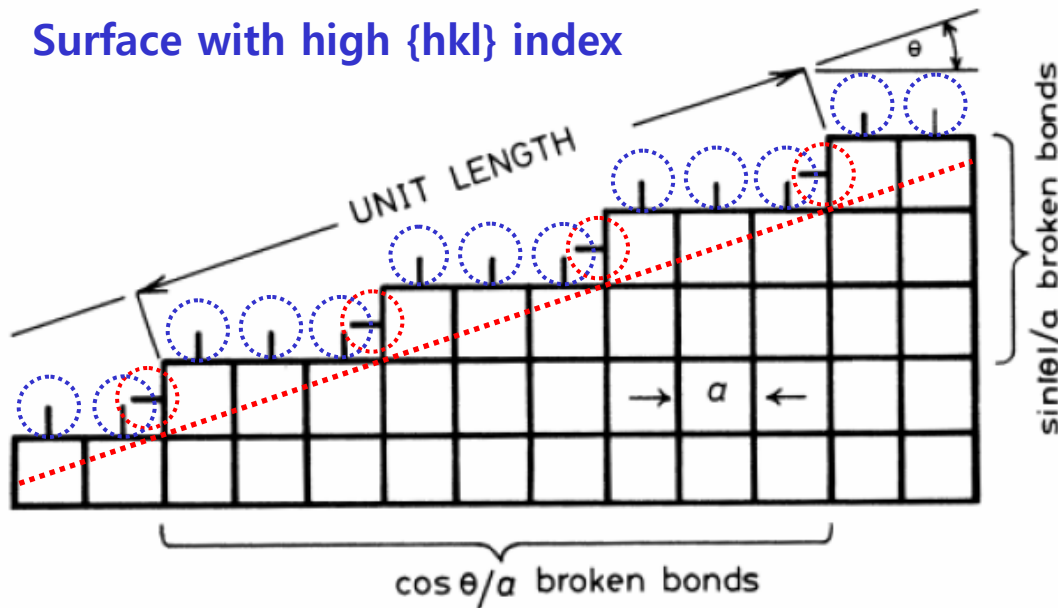


Fig. 3.3 The 'broken-bond' model for surface energy.

$(\cos\theta/a)(1/a)$: broken bonds
from the atoms on the steps

$(\sin|\theta|/a)(1/a)$: additional broken bonds
from the atoms on the steps

Surface energy for high or irrational {hkl} index

$(\cos\theta/a)(1/a)$: broken bonds from the atoms on the steps

$(\sin|\theta|/a)(1/a)$: additional broken bonds from the atoms on the steps

Attributing $\varepsilon/2$ energy to each broken bond,

$$E_{SV} = \frac{1}{1 \times a} \frac{\varepsilon}{2} \left(\frac{\cos \theta}{a} + \frac{\sin |\theta|}{a} \right)$$

$$= \frac{\varepsilon (\cos \theta + \sin (|\theta|))}{2a^2}$$

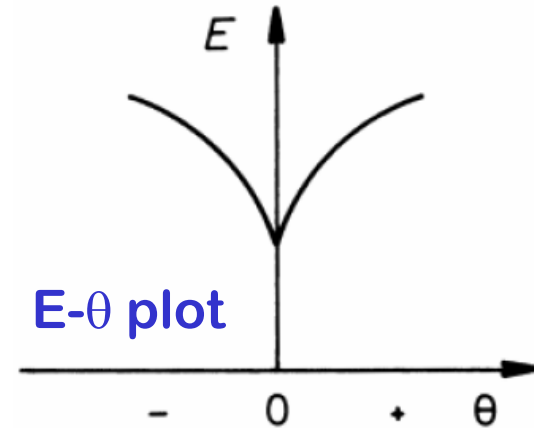


Fig. 3.4 Variation of surface energy as a function of θ

- **The close-packed orientation ($\theta = 0$) lies at a cusped minimum in the E plot.**
- Similar arguments can be applied to any crystal structure for rotations about any axis from any reasonably close-packed plane.
- **All low-index planes should therefore be located at low-energy cusps.**

Equilibrium shape of a crystal?

Equilibrium shape: Wulff surface

Distance from center : r_{sv}

Several plane A_1, A_2 etc. with energy γ_1, γ_2

Total surface energy : $A_1\gamma_1 + A_2\gamma_2 \dots$

$= \sum A_i \gamma_i \rightarrow \text{minimum}$

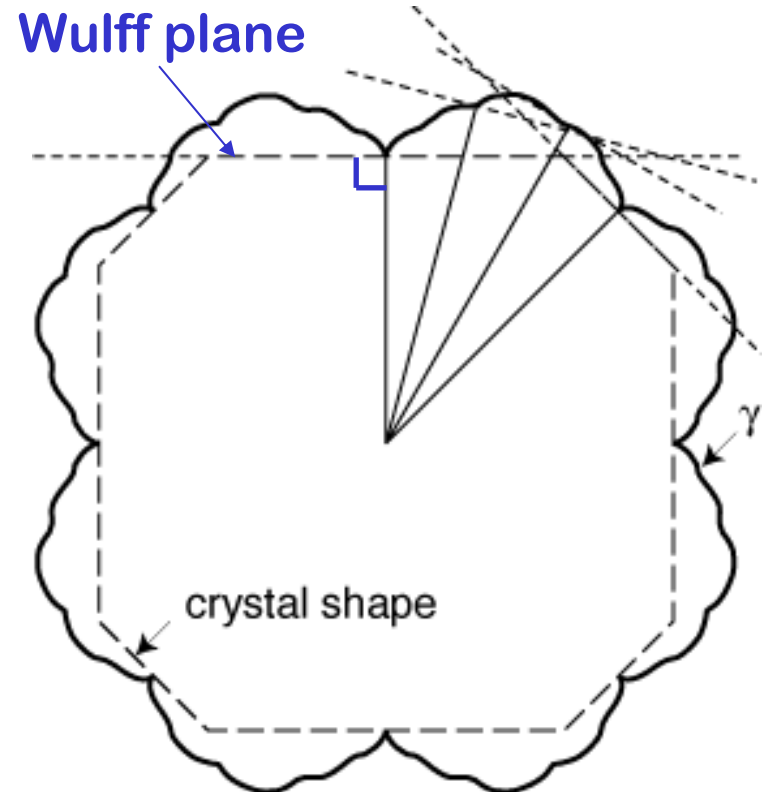
\rightarrow equilibrium morphology

단결정의 평형모형을 예측하는데 유용

Analytical solution in 2D is reported

How is the equilibrium shape determined?

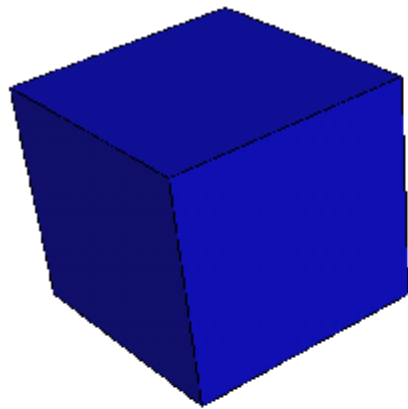
$$\gamma_j = \text{Minimum}$$



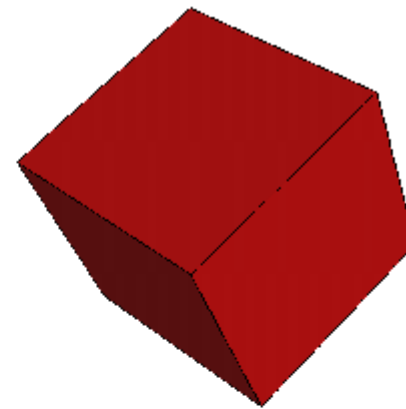
γ - θ plot

E_{sv} - θ diagram 보다 엔트로피 효과로 cusped minimum 발견 어려움.

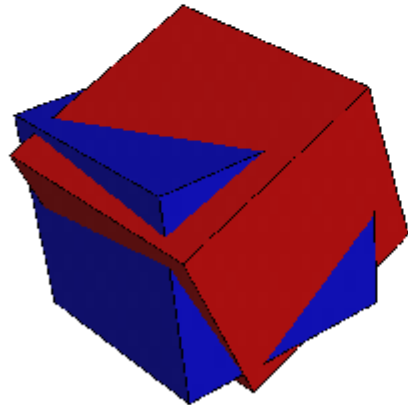
Process of Wulff shape intersection for two cubic wulff shapes



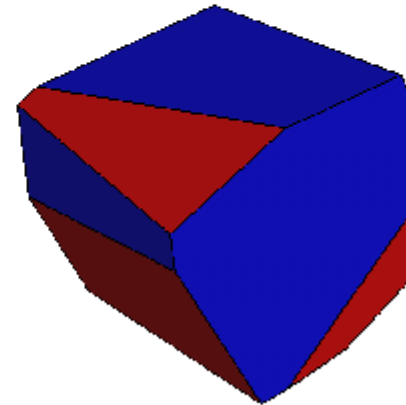
(a) Wulff Shape I



(b) Wulff Shape II



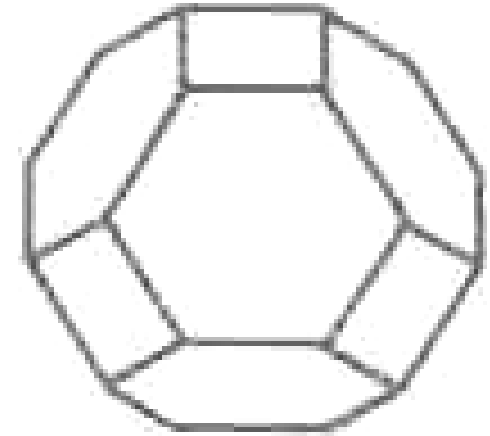
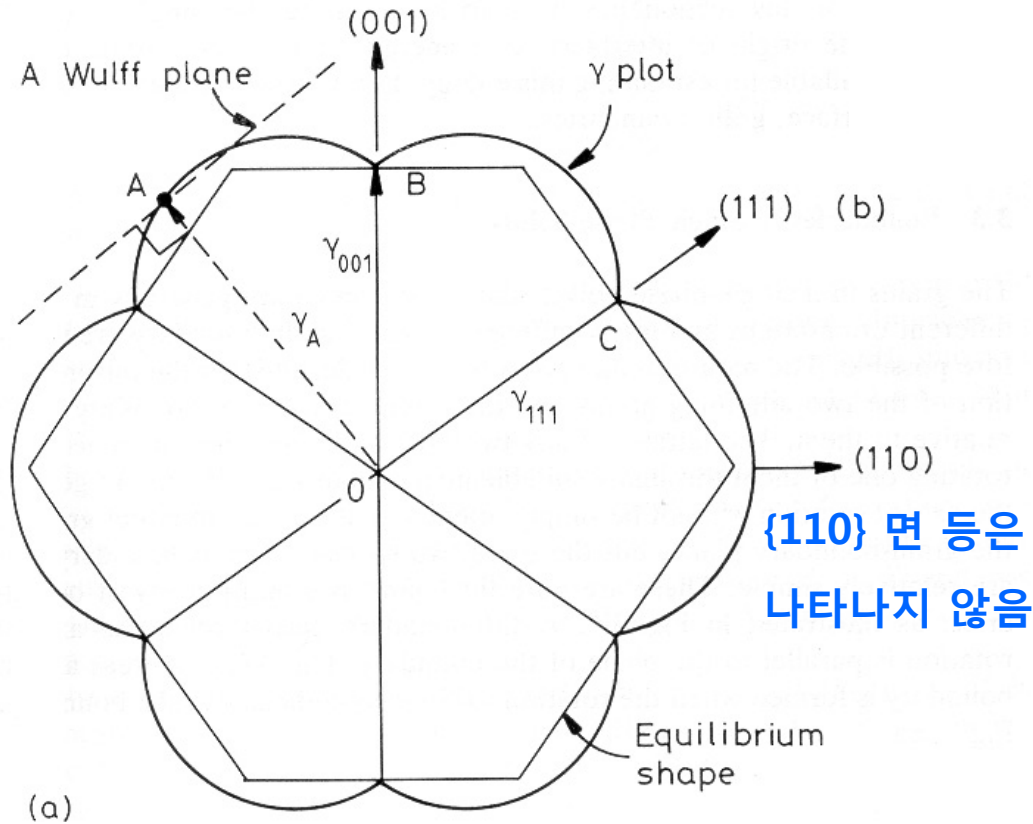
(c) Union of I and II



(d) Intersection of I and II

Figure 1: The process of Wulff shape intersection for two cubic Wulff shapes with displaced origins and rotated coordinate systems. Each individual shape has cubic symmetry $m\bar{3}m$ and $[100]$ facets.

Equilibrium shape: Wulff surface



FCC 금속의 평형모형

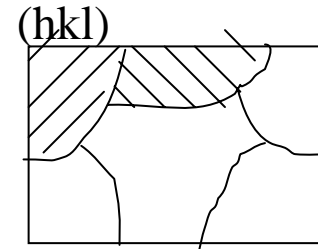
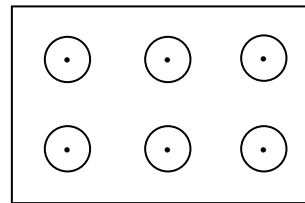
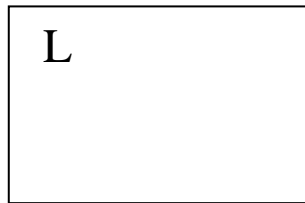
- 1) 정사각형의 {100} 과
- 2) 정육각형 {111}로 구성

Equilibrium shape can be determined experimentally by annealing small single crystals at high temperatures in an inert atmosphere, or by annealing small voids inside a crystal.

Of course **when γ is isotropic**, as for liquid droplets, both the γ -plots and equilibrium shapes are **spheres**.

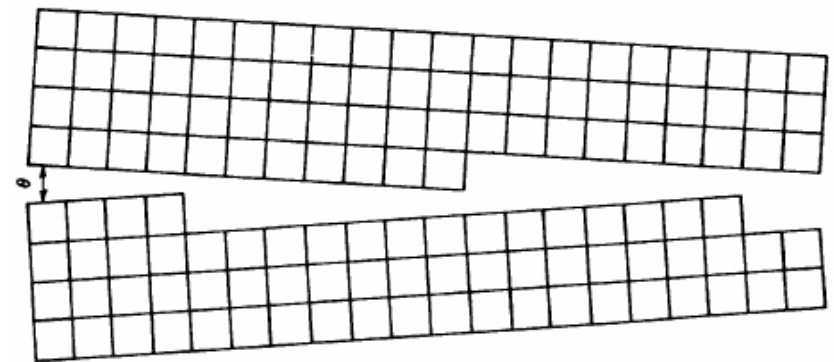
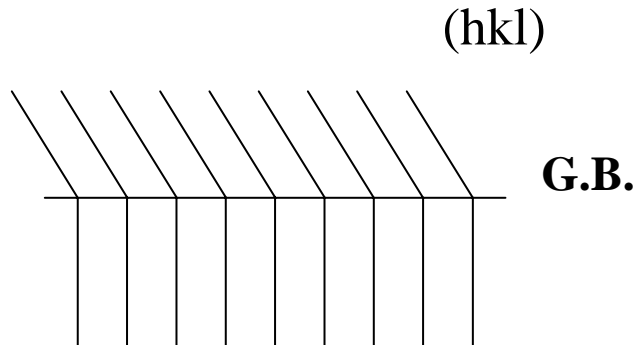
3.3 Boundaries in Single-Phase Solids

Grain boundary (α/α interfaces)



> same composition, same crystal structure

> different orientation



1) misorientation of lattice in two grains

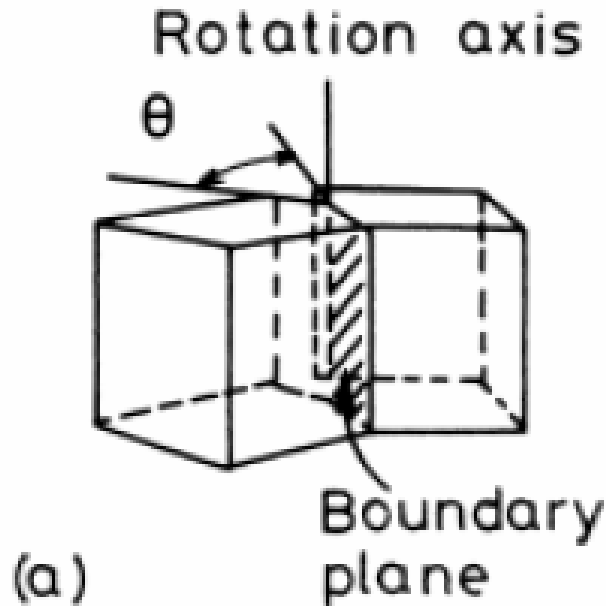
두 개 인접한 결정립의 방위차이

2) orientation of grain boundary

인접 결정립과 입계면의 방위관계

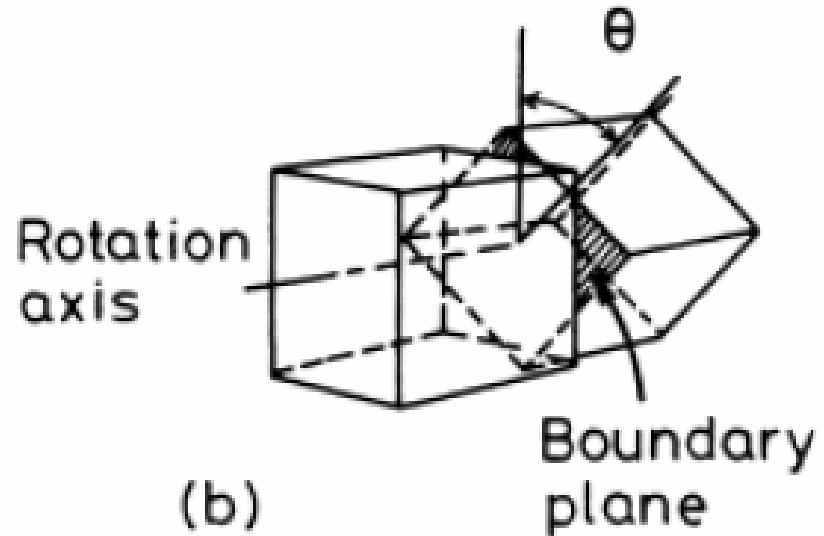
3.3 Boundaries in Single-Phase Solids

두 결정립 격자 단일축을 중심으로 적당한 각으로 회전시 일치됨.



tilt boundary

$\theta \rightarrow$ misorientation
 \rightarrow tilt angle



twist boundary

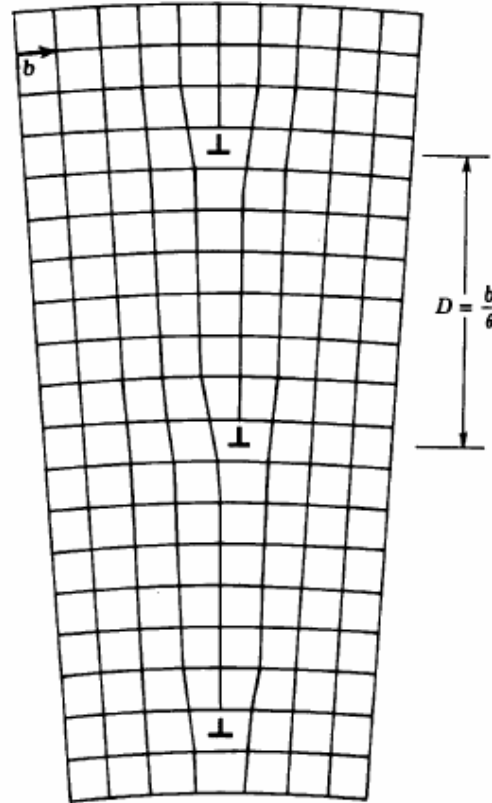
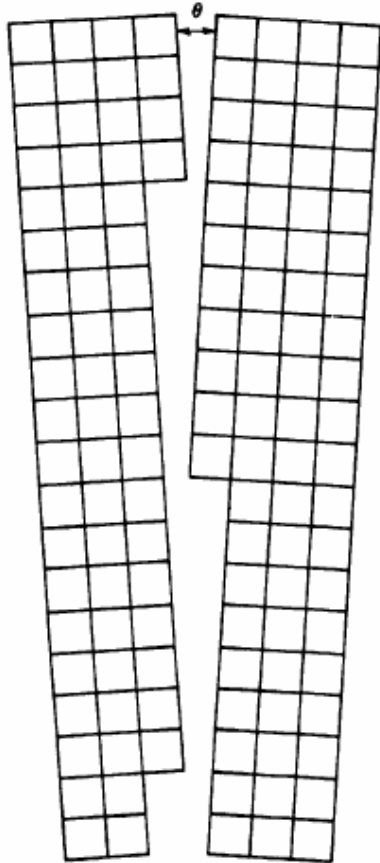
$\theta \rightarrow$ misorientation
 \rightarrow twist angle

[symmetric tilt or twist boundary
non-symmetric tilt or twist boundary

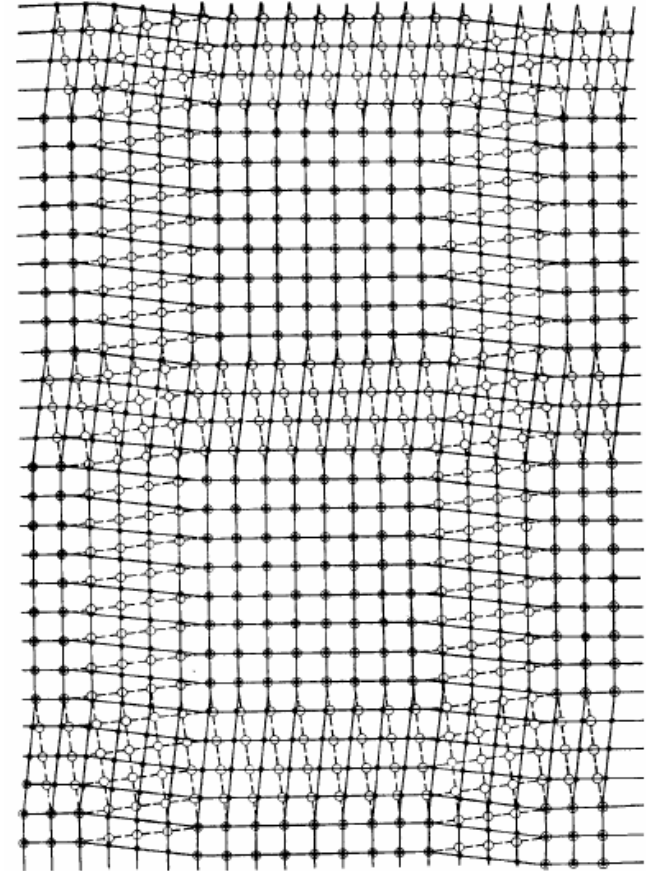
3.3.1 Low-Angle and High-Angle Boundaries

Low-Angle Boundaries

Symmetrical low-angle tilt boundary



Symmetrical low-angle twist boundary



(a)

Fig. 3.7 (b)

Fig. 3.7 (a) Low-angle tilt boundary, (b) low-angle twist boundary: ○ atoms in crystal below, ● atoms in crystal above boundary. (After W.T. Read Jr., *Dislocations in crystals*, McGraw-Hill, New York, 1953.)

평행한 칼날전위의 배열

서로 직교하는 나선전위들의 배열 ²¹

tilt Boundaries

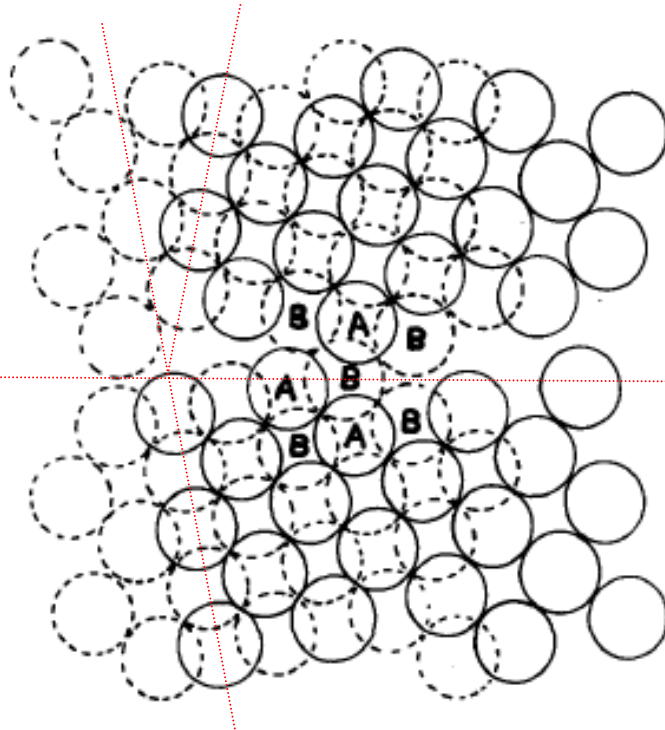
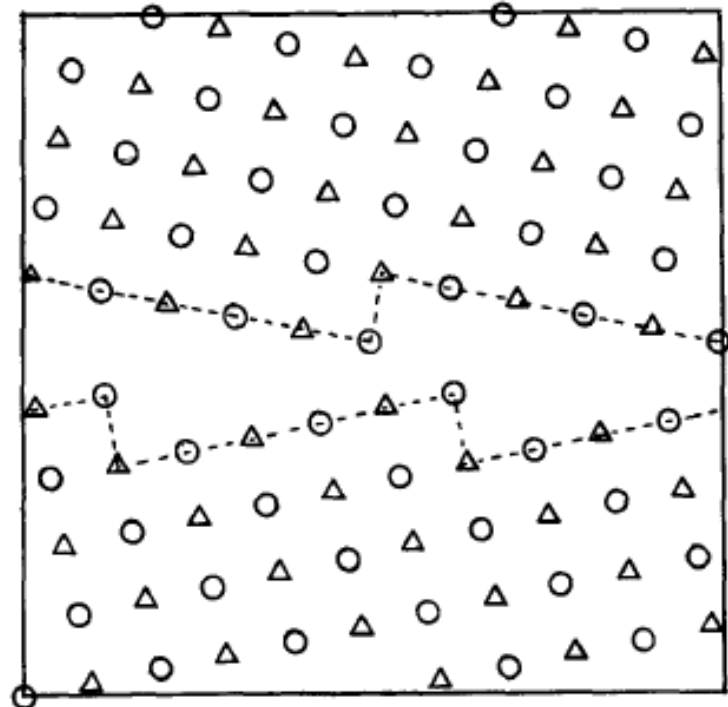
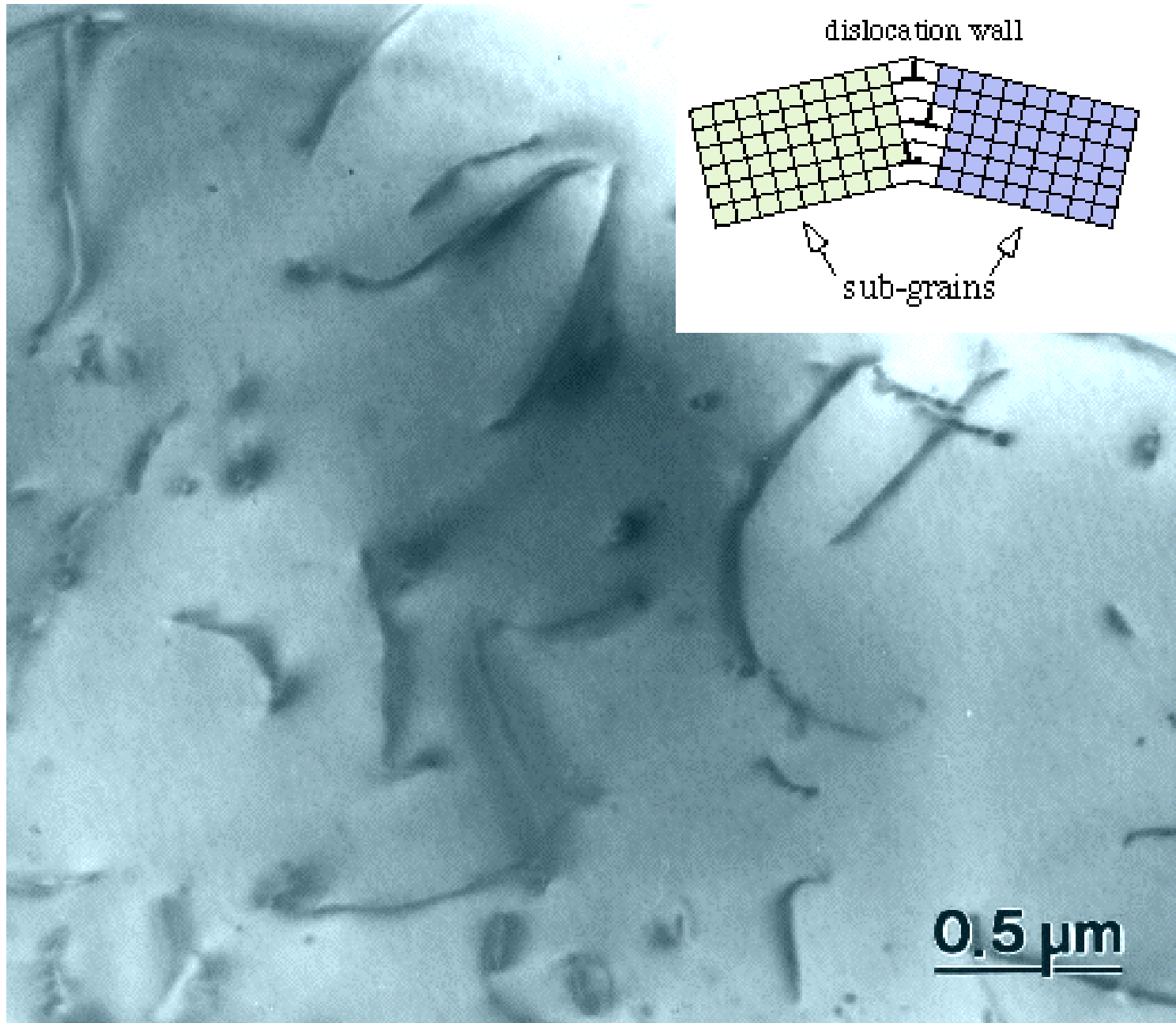


Figure 1 - 23° symmetric tilt boundary about a $\langle 001 \rangle$ axis. The circles with dashed lines represent one layer and the circles with solid lines the other layer of the AB...stacked $\{001\}$ planes. The atoms labelled A and B denote the structural unit.

Figure 2 - 23° symmetric tilt boundary about a $\langle 001 \rangle$ axis. Δ represent one layer and \circ represent the other layer of the AB..... stacked $\{001\}$ planes. The ledge like character of the boundary is shown by the dashed lines.



Dislocations



twist Boundaries

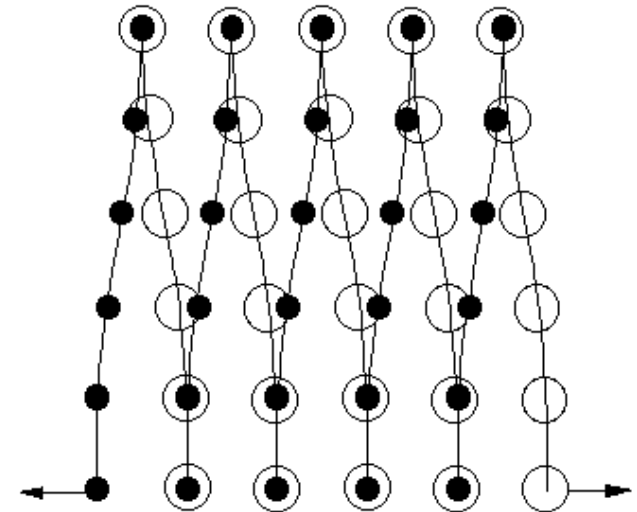
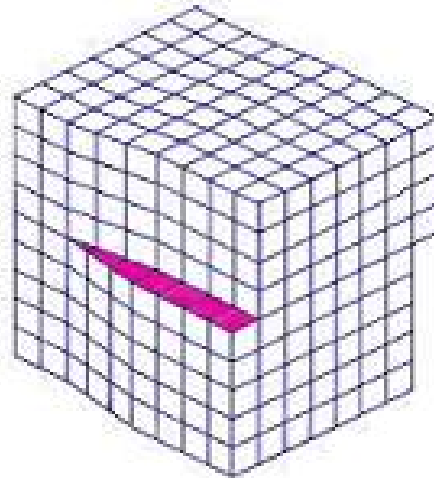
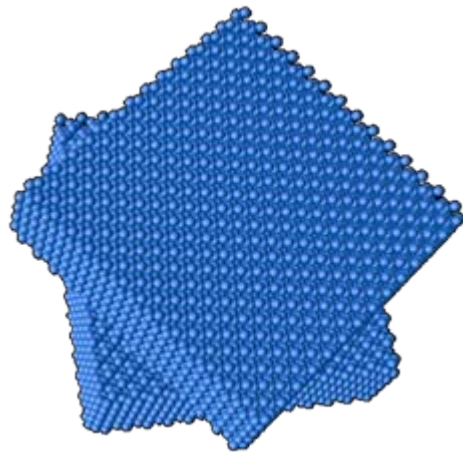
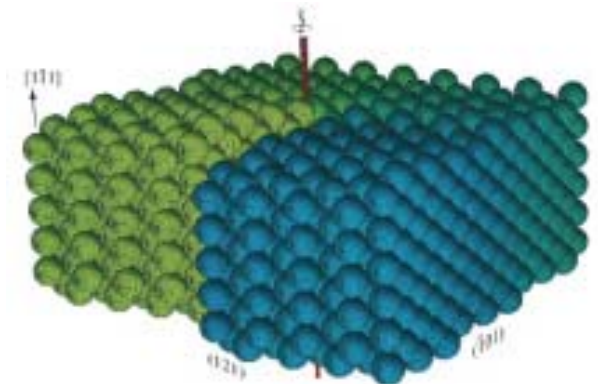
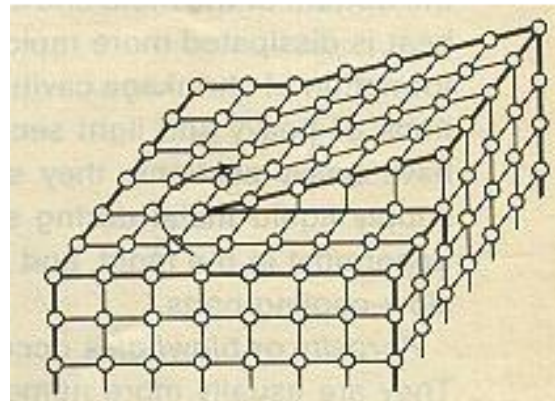
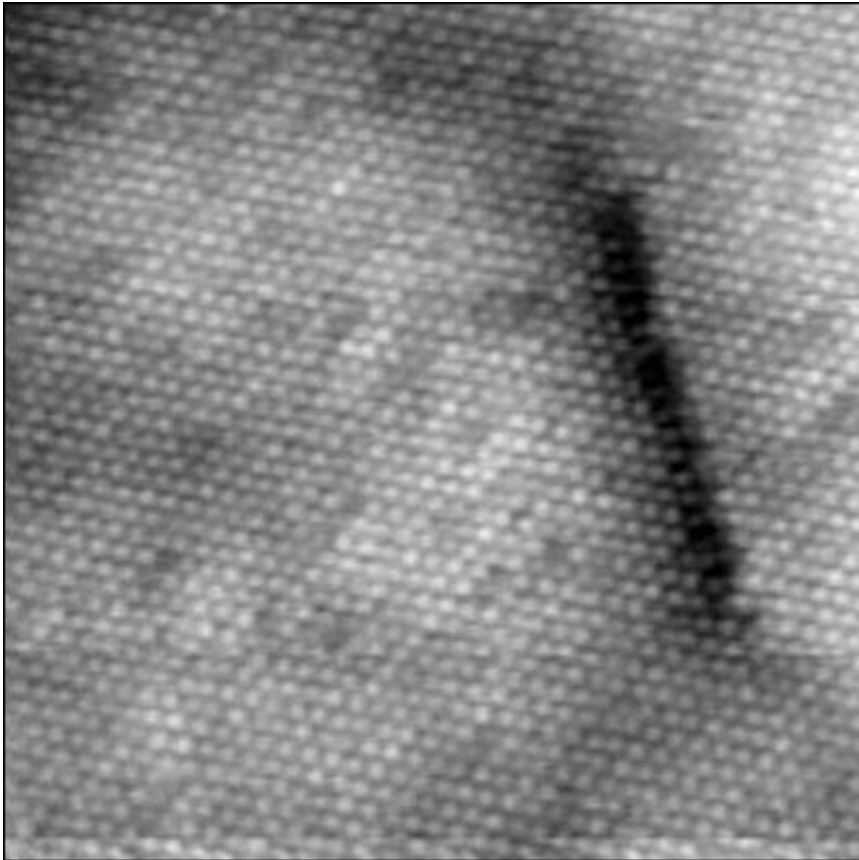


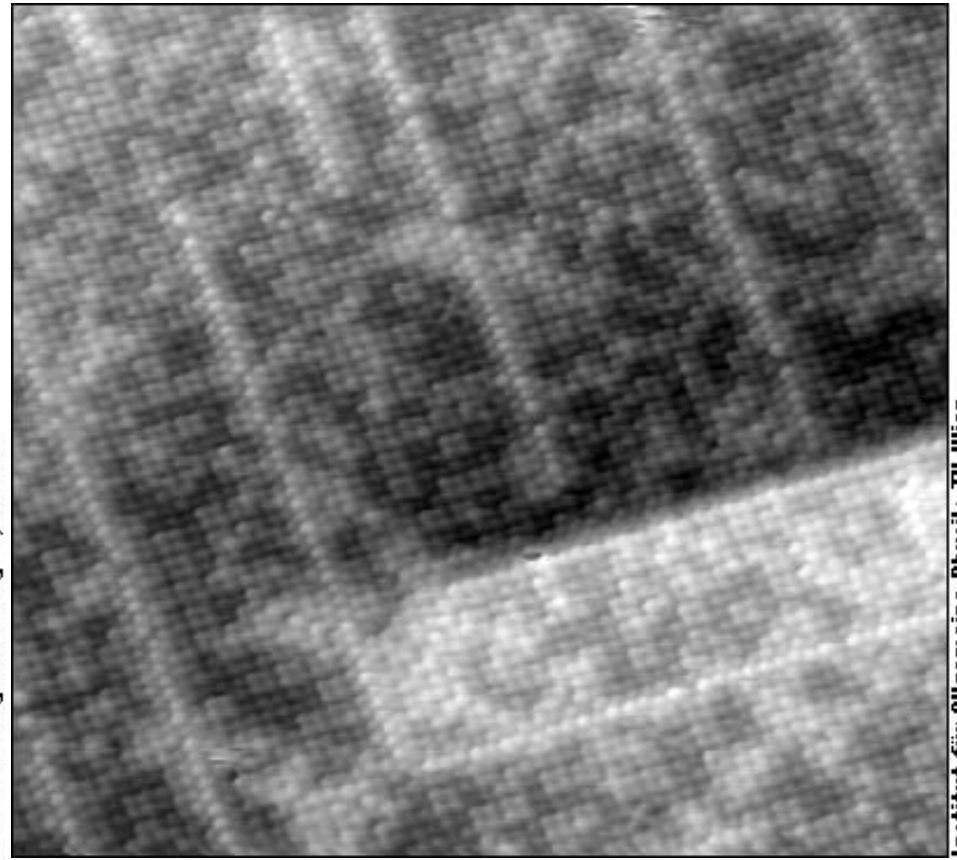
Figure 2. A screw dislocation; note the screw-like 'slip' of atoms in the upper part of the lattice



Screw dislocation

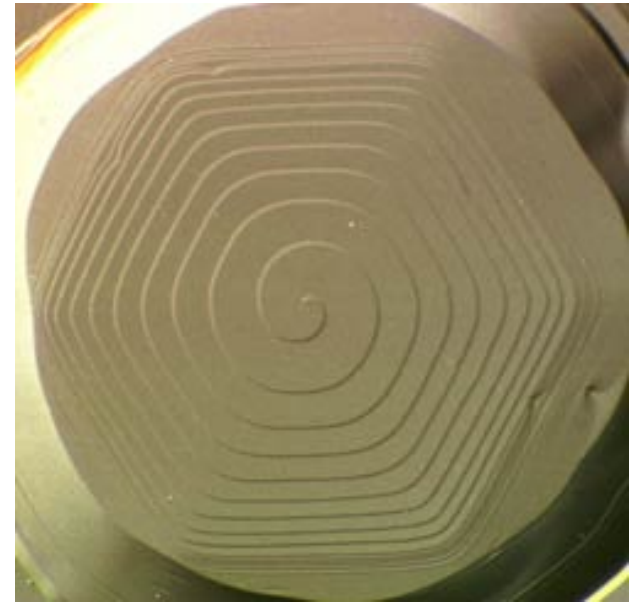
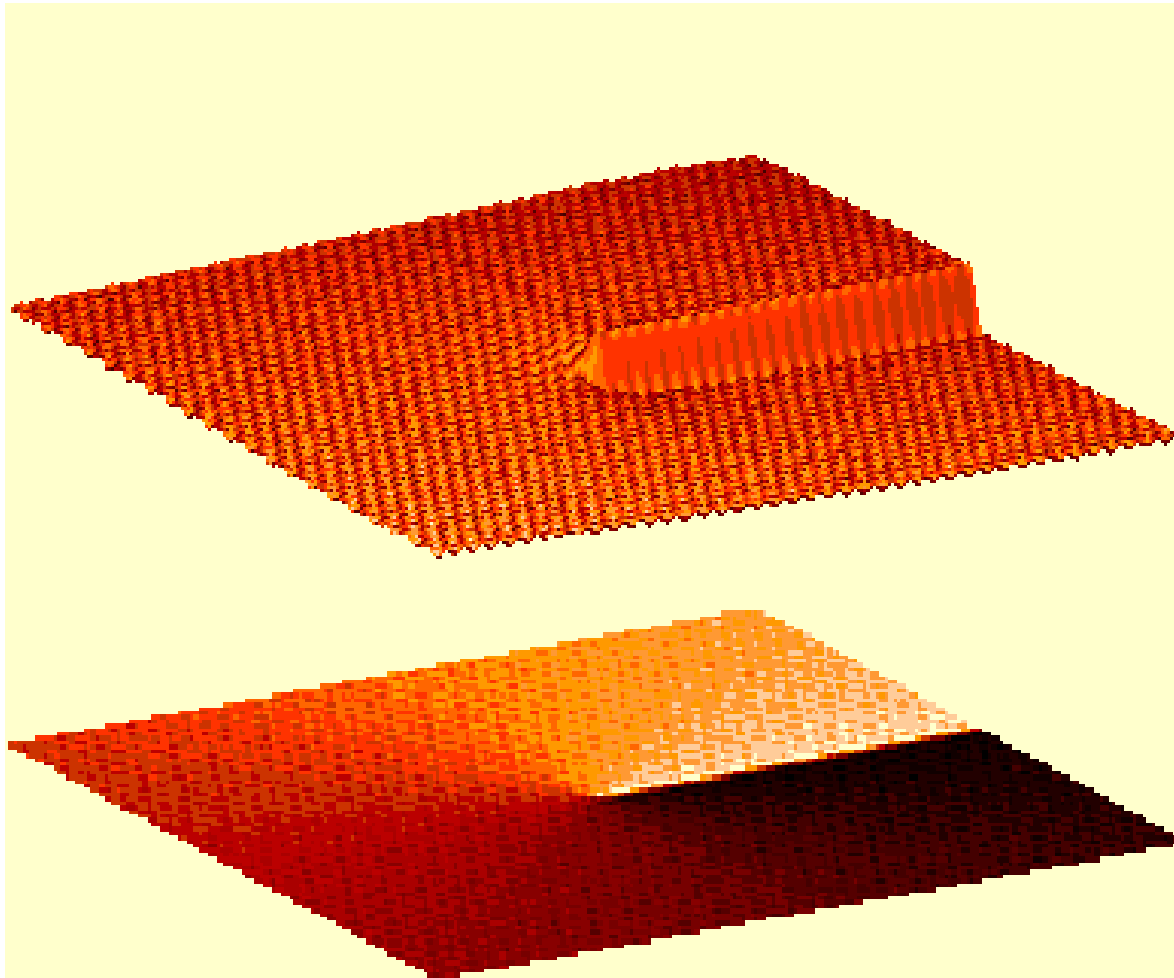


Institut für Allgemeine Physik, TU Wien

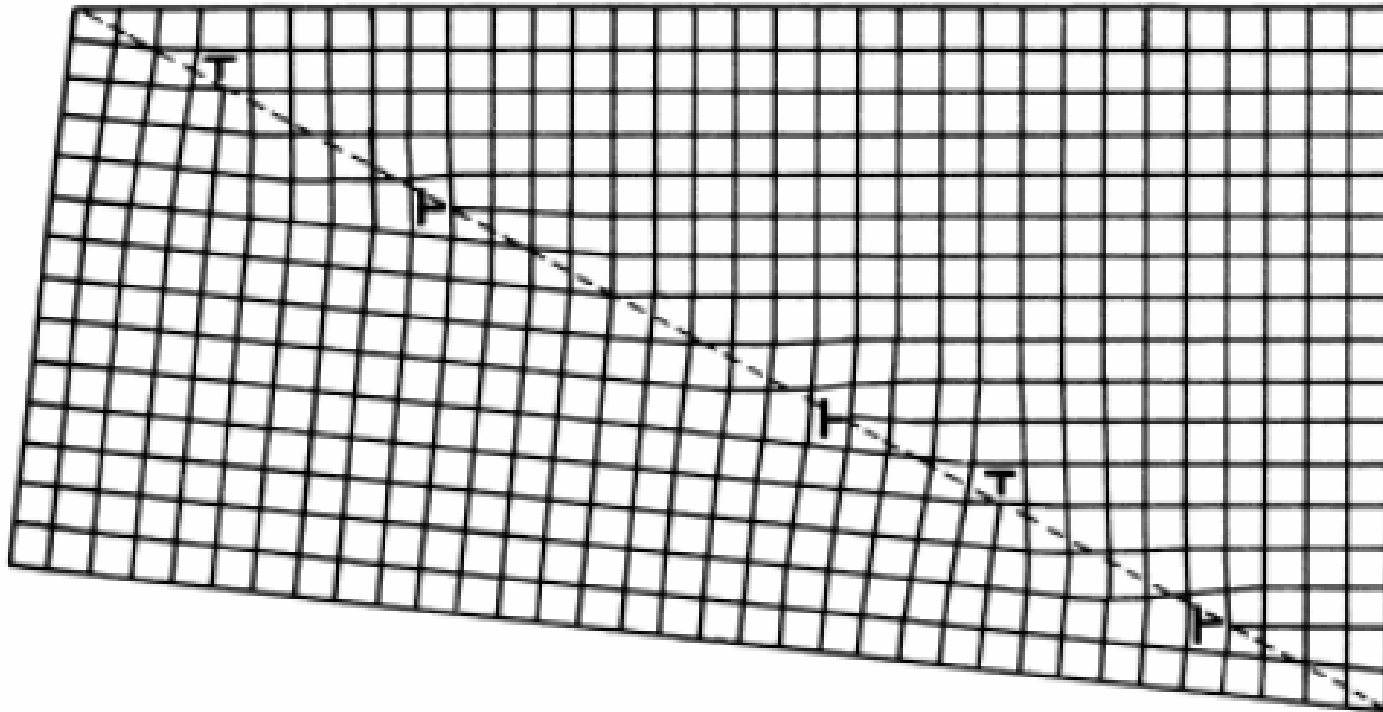


Institut für Allgemeine Physik, TU Wien

Growth of Screw dislocation



Non-symmetric Tilt Boundary



vectors are present. (After W.T. Read Jr., *Dislocations in Crystals*, McGraw-Hill, New York, 1953.)

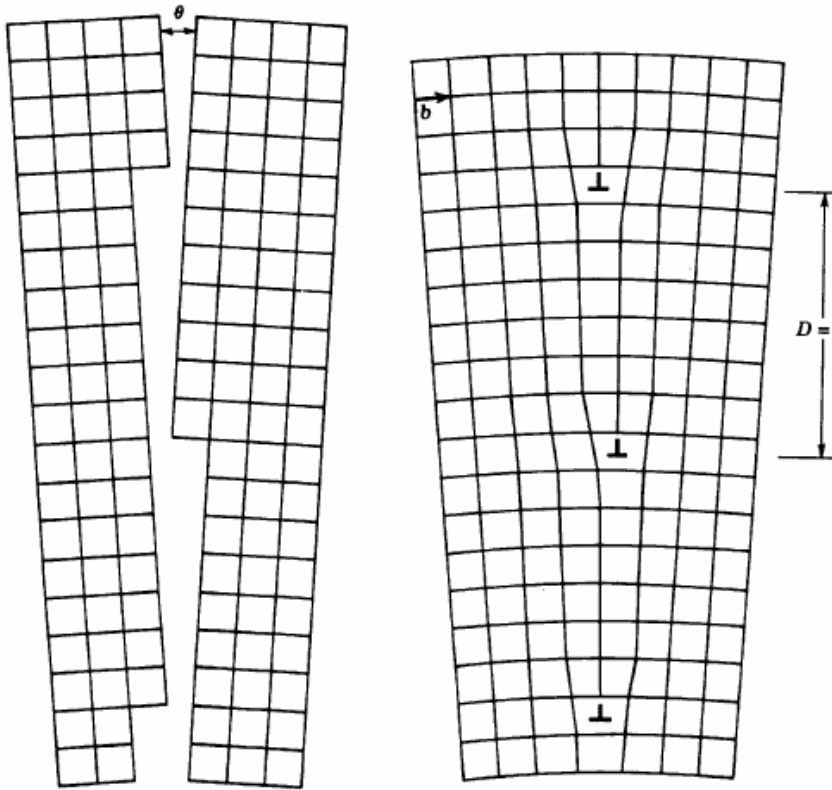
If the boundary is unsymmetrical, dislocations with different Burgers vectors are required to accommodate the misfit.

In general boundaries of a mixture of the tilt and twist type, → several sets of different edges and screw dislocations.

3.3.1 Low-Angle and High-Angle Boundaries

Low-Angle tilt Boundaries

→ around edge dislocation : strain ↑
 but, LATB ~ almost perfect matching



전위의 버거스 벡터

양쪽 결정의 방위차

$$\sin \frac{\theta}{2} = \frac{b/2}{D}$$

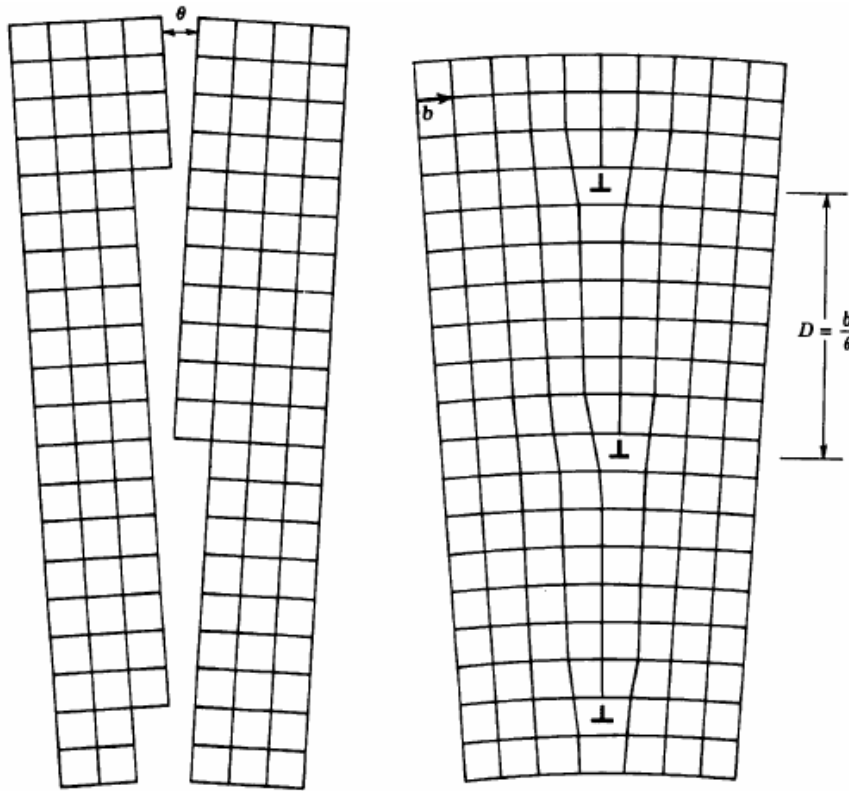
$$\sin \frac{\theta}{2} \approx \frac{\theta}{2}$$

$$D \cong \frac{b}{\theta}$$

소각 경계 에너지 ~ 입계의 단위면적 안에 있는 전위의 총 에너지
 ~ 전위의 간격 (D)에 의존

3.3.1 Low-Angle and High-Angle Boundaries

Low-Angle tilt Boundaries



→ around edge dislocation : strain ↑
 but, LATB ~ almost perfect matching

→ g.b. energy : $\gamma_{g.b.} \rightarrow E / \text{unit area}$
 (energy induced from dis.)

* Relation between D and γ ?

$\sin\theta = b/D$, at low angle θ 가 매우 작은 경우
 D가 매우 크다.

→ $D=b/\theta \rightarrow \gamma_{g.b.}$ is proportional to $1/D$

→ low angle tilt boundary

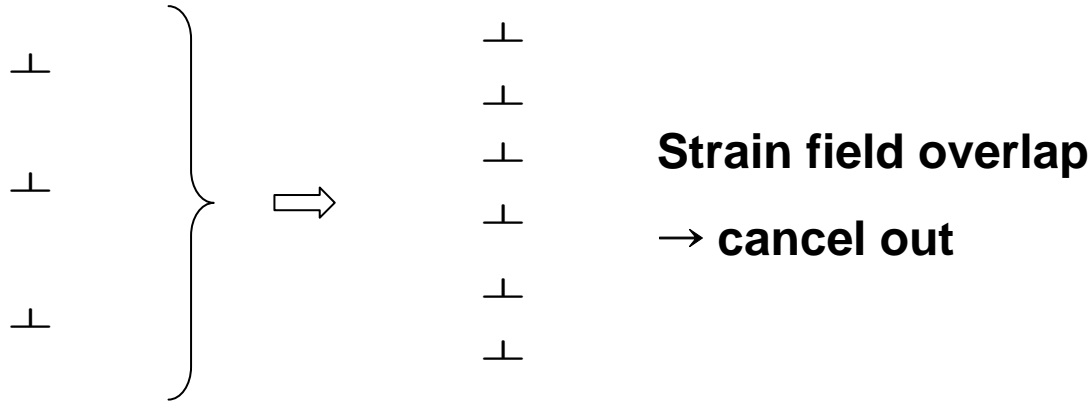
→ Density of edge dis.

$$\gamma \propto \theta$$

(cf. low angle twist boundary → screw dis.)

Low-Angle tilt Boundaries

⇒ 1) As θ increases, $\gamma_{g.b.}$ ↑

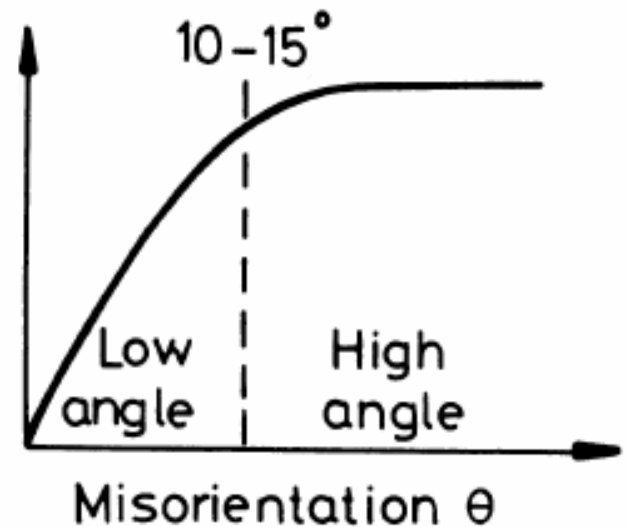


→ 2) $\gamma_{g.b.}$ increases and the increasing rate of γ ($=d\gamma/d\theta$) decreases.

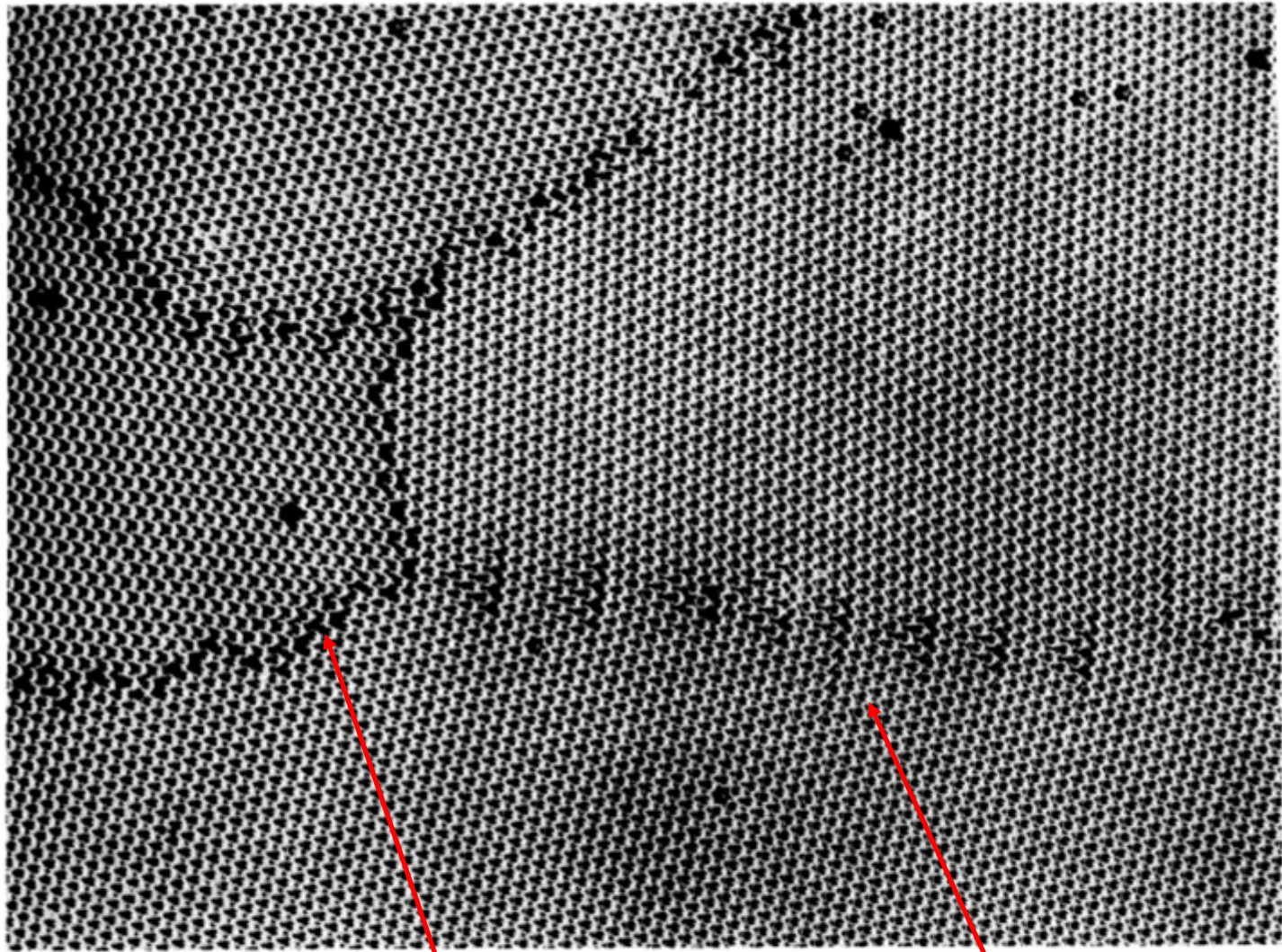
→ 3) if θ increases further, it is impossible to physically identify the individual dislocations

→ 4) increasing rate of $\gamma_{g.b.} \sim 0$

Grain boundary
Energy γ



5) 전위간격이 너무 작아 전위의 구별이 불가능해지고,
결정립계 에너지가 방위차와 무관해짐.



전위구별 가능

Fig. 3.11 Rafts of soap bubbles showing several grains of varying misorientation. Note that the boundary with the smallest misorientation is made up of a row of dislocations, whereas the high-angle boundaries have a disordered structure in which individual dislocations cannot be identified. (After P.G. Shewmon, *Transformations in Metals*, McGraw-Hill, New York, 1969, from C.S. Smith.)

무질서해서 전위구별 불가능

High Angle Grain Boundary

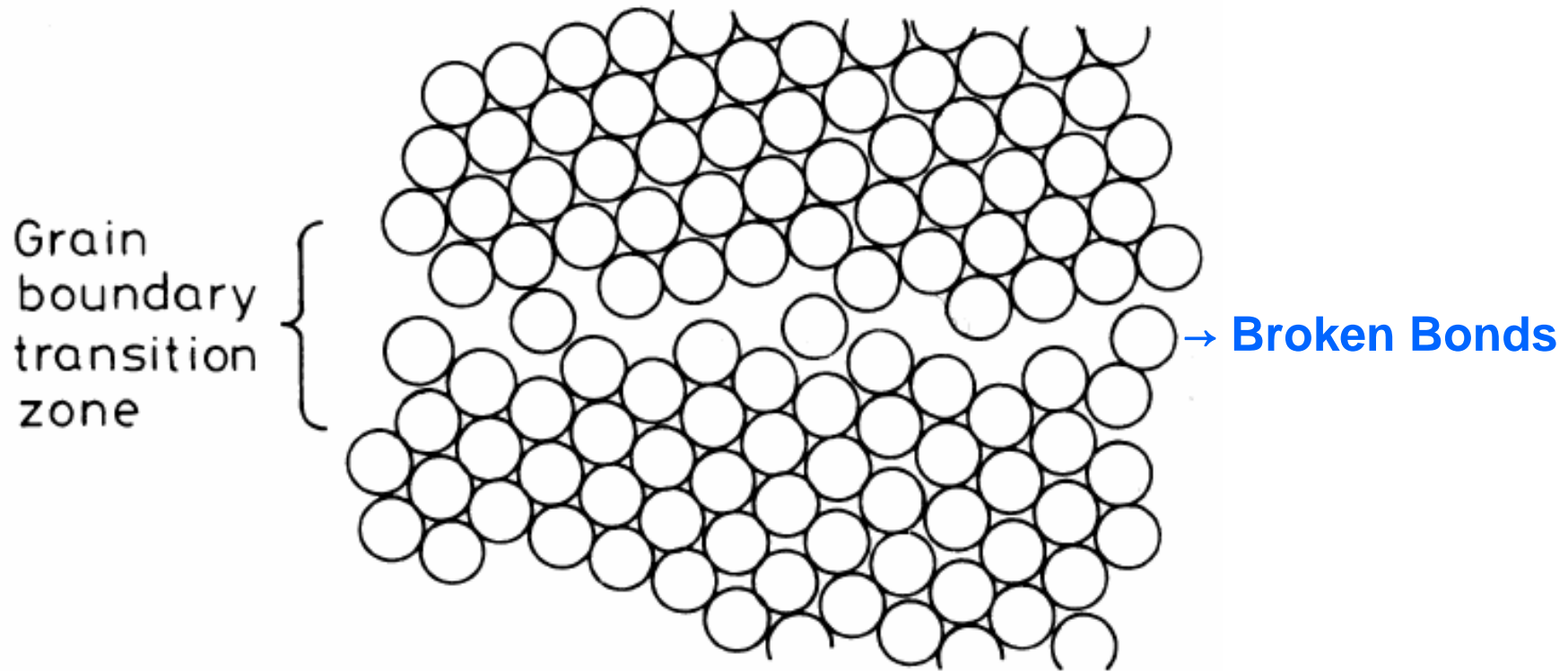


Fig. 3.10 Disordered grain boundary structure (schematic).

High angle boundaries contain large areas of poor fit and have a relatively open structure.

→ high energy, high diffusivity, high mobility (cf. segregated gb)

High Angle Grain Boundary

Low angle boundary

→ almost perfect matching (except dislocation part)

High angle boundary (almost)

→ open structure, large free volume

* low and high angle boundary

high angle $\gamma_{g.b.} \approx 1/3 \gamma_{sv}$ → Broken Bonds

Measured high-angle grain boundary energies

Crystal	$\gamma_b / \text{mJ m}^{-2}$	T/°C	γ_b / γ_{sv}
Sn	164	223	0.24
Al	324	450	0.30
Ag	375	950	0.33
Au	378	1000	0.27
Cu	625	925	0.36
γ -Fe	756	1350	0.40
δ -Fe	468	1450	0.23
Pt	660	1300	0.29
W	1080	2000	0.41

E_{sv} 처럼 γ_b 도 온도 증가시 감소하는 온도의존형

